ChemComm

COMMUNICATION

View Article Online
View Journal | View Issue

Cite this: *Chem. Commun.*, 2021, **57**, 3995

Received 3rd February 2021,
Accepted 15th March 2021

DOI: 10.1039/d1cc00627d

rsc.li/chemcomm

De novo approach for the synthesis of water-soluble interlocked and non-interlocked organic cages†

Debsena Chakraborty,‡ Ritwik Modak,‡ Prodip Howlader and Partha Sarathi Mukherjee *

Research on self-assembled metallosupramolecular architectures has bloomed in recent times. Analogous metal–free organic architectures with water solubility are highly challenging. We report here a unique class of triazine based immidazolium water-soluble metal–free interlocked organic cage (1), which was synthesized in a one-pot reaction without using dynamic covalent chemistry and without any chromatographic separation. An analogous non-interlocked cage (2) was also successfully achieved by steric control using different positional isomers of the building blocks.

Mechanically interlocked molecules (MIMs) are a class of molecules that have multiple molecular fragments connected not by covalent bonding but through bond topology, such that the fragments cannot be separated from each other without breaking chemical bonds. Such interlocked systems are not just aesthetically beautiful but also find applications.[1] In nature too, a myriad of interlocked molecules[2,3] are used for different life processes. To obtain more insight into natural processes, artificial analogues are often created that help in better understanding the role of such topologies.[4,5] The requirement thus for proper biomimetic MIMs is that they should be robust and soluble in water. To make such molecules, the most prevalent approach is to use dynamic combinatorial chemistry (DCC) where reversible metal–ligand[6–9] and dynamic covalent bonds[10–12] are employed to obtain the thermodynamically most stable product. Using such processes, several structures like Borromean rings,[13] Solomon's knots[14] and interlocked cages/3D catenanes[15–18] have been synthesised. However, because of the dynamic nature of such reactions the products formed are always associated with a small window of stability. Thus, MIMs formed using such reactions are not chemically stable over a wide range of pH or solvent concentrations. Furthermore, a few metal–based assemblies have the added disadvantage of being toxic towards biological systems. On the other hand, self-assembly employing dynamic covalent chemistry yields products that are either insoluble or labile in an aqueous medium. The best approach is thus to use covalent bond forming reactions to obtain charged organic systems based on the pyridinium or imidazolium moieties. Such techniques have been used by others[19,20] to obtain charged macrocycles that were later used to obtain rotaxanes and catenanes. Although both the pyridinium and imidazolium cages[21] are known, they are rare, and no instance of a water-soluble charged interlocked cage has been reported so far.

Herein, we report a water-soluble charged imidazolium interlocked cage and show how changing the steric environment of the building blocks can lead to a non-interlocked cage. To make such systems we used the concept of preorganisation, which is often used in self-assembly to get high yielding products.[22] Thus two precursors $\mathbf{L_1}$ [2,4,6-tris(4-(bromomethyl)-phenyl)-1,3,5-triazine] and $\mathbf{L_2}$ [2,4,6-tris(4-((1*H*-imidazol-1-yl)methyl)phenyl)-1,3,5-triazine] bearing a triazine core were treated in a 1 : 1 ratio to obtain an interlocked cage **1** (Scheme 1). Such an interlocked architecture within the confinements of such a small pocket is very interesting. To understand the dynamics of the formation of such an interlocked architecture we changed the steric environment around the building units and found that by using the meta isomers $\mathbf{L_3}$ [2,4,6-tris(3-(bromomethyl)phenyl)-1,3,5-triazine] and $\mathbf{L_4}$ [2,4,6-tris(3-((1*H*-imidazol-1-yl)methyl)phenyl)-1,3,5-trizine] a non-interlocked cage **2** (Scheme 1) could be synthesised. To the best of our knowledge such correlation in interlocked cyclophane formation is new.

$\mathbf{L_1}$ was synthesized by cyclotrimerization of 4-(bromomethyl)benzonitrile, and $\mathbf{L_2}$ was prepared *via* a base mediated coupling of imidazole with $\mathbf{L_1}$. To make the imidazolium cage from these two building units, a $CHCl_3/CH_3CN$ (4 : 1) solution of $\mathbf{L_2}$ (0.47 mM) containing 3 equivalents of TBAI (tetra *n*-butylammonium iodide) was added dropwise over a period of

Department of Inorganic and Physical Chemistry, Indian Institute of Science, Bangalore-560012, India. E-mail: psm@iisc.ac.in

† Electronic supplementary information (ESI) available: Synthesis, NMR, ESI-MS spectra and optimized structures. See DOI: 10.1039/d1cc00627d

‡ Debsena Chakraborty and Ritwik Modak contributed equally.

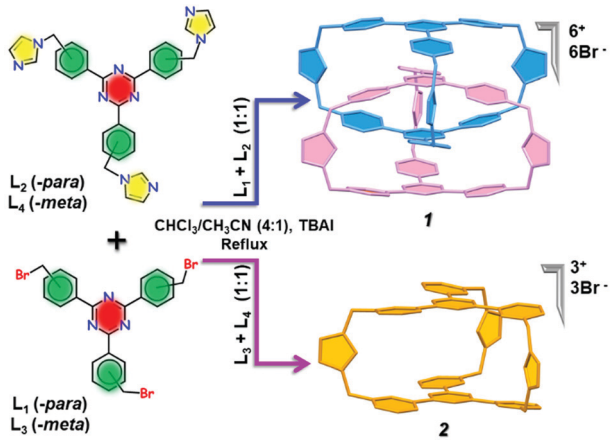

Scheme 1 Selective synthesis of the interlocked cage **1** and non-interlocked cage **2**.

6–8 hours to an equimolar solution of $\mathbf{L_1}$ in $CHCl_3/CH_3CN$ (4 : 1). The resultant white precipitate was collected *via* centrifugation after four days of refluxing this mixture (yield: 26%). The ^{1}H NMR spectrum of the product in D_2O showed nine peaks (Fig. 1 and Fig. S1, ESI†). However, the ^{1}H DOSY NMR spectrum showed that all peaks correspond to the same diffusion coefficient [$D = 2.51 \times 10^{-10}$ m^2 s^{-1} (log $D = -9.6$)] (Fig. S2, ESI†), suggesting the formation of a single assembly. A [1+1] self-assembled non-interlocked imidazolium cage would have only five peaks. Due to the complex nature of ^{1}H NMR, we started investigating the possibility of an interlocked system or a more complex architecture. To understand the kind of assembly formed, ^{1}H COSY and NOESY NMR of the same solution were studied to assign all peaks (Fig. S3 and S4, ESI†). The COSY NMR showed clear correlation between the H_a, H_b and $H_{a'}$, $H_{b'}$ peaks. It showed that the resonance of $H_{a'}$, $H_{b'}$ is significantly up-field shifted compared to that of H_a, H_b, which can be caused due to the shielded surrounding of an interlocked cavity. The NOESY spectrum showed NOE between the H_a and $H_{a'}$ peaks, and such a correlation would suggest that the two peaks are spatially close

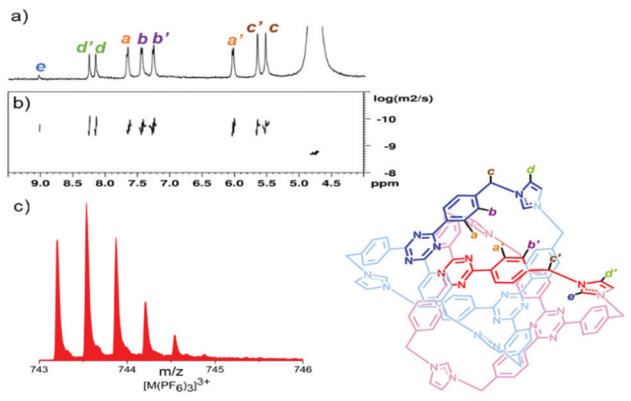

Fig. 1 (a) The ^{1}H NMR spectrum of **1** (D_2O). (b) The ^{1}H DOSY NMR spectrum of **1**. (c) Experimental isotopic distribution patterns of the ESI-MS peak corresponding to the $[M(PF_6)_3]^{3+}$ (where M = molar mass of $\mathbf{1}^{6+}$) fragments in acetonitrile.

which is not possible in a regular structure and can only happen if an interlocked geometry is formed. To further validate the claim of an interlocked cage (**1**), ^{13}C NMR and ESI-MS were carried out (Fig. S6–S10, ESI†) on the PF_6^- salt of **1**. The ^{13}C NMR spectrum showed the presence of fifteen peaks which can be attributed to the systematic splitting of all carbon peaks into two sets, a phenomenon seen widely in interlocked systems.[23]

The ESI-MS spectrum of the PF_6^- salt showed a peak at m/z = 743.5562, corresponding to the fragment $[M(PF_6)_3]^{3+}$ with a proper isotopic distribution pattern. This confirms the presence of two units of both $\mathbf{L_1}$ and $\mathbf{L_2}$ in **1**. Two possible structures can be formed from two units of $\mathbf{L_1}$ and $\mathbf{L_2}$: (a) a double-square cage and (b) an interlocked cage (Scheme 2). Both the structures would show systematic peak splitting but the splitting pattern in the double-square cage will be 2 : 1 (*i.e.*, H_a hydrogens would have integration in the ^{1}H spectra twice that of $H_{a'}$ or *vice versa*). But, in the case of an interlocked cage, the peak splitting of ^{1}H peaks should be 1 : 1 (*i.e.*, H_a hydrogens would have the same integration in the ^{1}H spectrum as $H_{a'}$), which matched nicely with the experimental results. No suitable single crystals for X-ray diffraction could be obtained. All above experimental data indicate the formation of an interlocked cage, which was stable for several weeks in an aqueous medium.

The DFT optimized structure of the interlocked cage was obtained at the B3LYP/6-31G level (Fig. 2). The optimized structure shows that the π–π interaction between the triazine cores mainly stabilizes the interlocked structure. Two triazine cores are separated by *ca.* 3.4 Å. This interpenetration inevitably causes each of the trigonal platforms to blow outward from planarity. To understand the extent of swelling up the cage is undergoing because of interlocking, we optimized a hypothetical free cage with the same building blocks. Comparing the distance between the triangular faces (floor and roof) of the hypothetical cage to that of **1** (Fig. S22 and S23, ESI†) showed that the molecule swelled up by *ca.* 1.2 Å. Such swelling of the cage is unique in the imidazolium systems. To understand the driving force responsible for the formation of an interlocked structure, we took a closer look into the mechanism of formation of different known interlocked systems.[24]

In most of the interlocked cage formation mechanisms, first the non-interlocked free cage is formed, and then it encapsulates a building unit, through which another cage is formed, making the whole system interlocked. This however will not be the case in our system as the formation of an imidazolium cage would

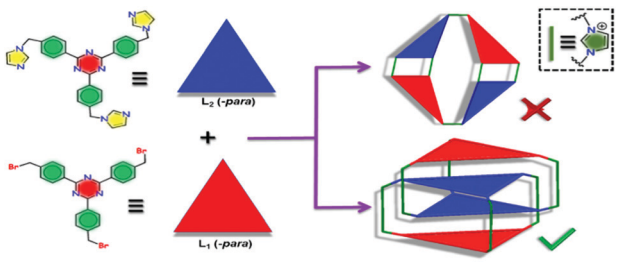

Scheme 2 Possible structures of the [2+2] assembly of $\mathbf{L_1}$ and $\mathbf{L_2}$.

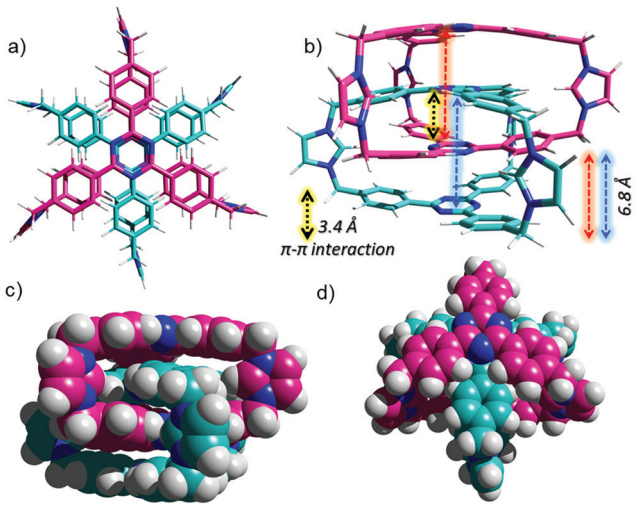

Fig. 2 Optimised structure of **1**: (a) top view, (b) side view, (c) side view (space filled model), and (d) top view (space filled model). The pink and cyan atoms denote carbon atoms of two different cages. The white and blue atoms denote hydrogen and nitrogen, respectively.

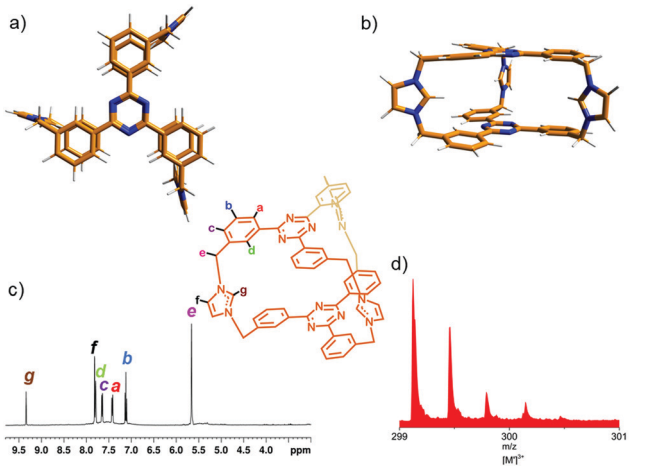

Fig. 3 Optimized structure of **2**: (a) top view, (b) side view, and (c) ^{1}H NMR spectrum of **2** (CD_3CN). (d) Experimental isotopic distribution patterns of the peaks corresponding to $[M']^{3+}$ (where M′= molar mass of $\mathbf{2}^{3+}$) fragments in acetonitrile. [Orange, white, and blue atoms denote C, H and N, respectively].

cause the system to precipitate out from the reaction mixture stopping further reaction.[21] The mechanism of choice should have all six imidazolium rings forming simultaneously. This is possible if the transition state itself is a preorganised π–π stacked model bearing a very close structural resemblance to that of the final product (**1**) such that forming six imidazolium rings directly leads to **1**. Understanding that the π–π interactions are the main driving forces behind the formation of such an intriguing system, we wanted to see what would happen if we disrupted the stacking by introducing a guest molecule. The guest molecule of choice was 2,4,6-triphenyl-1,3,5-triazine (**TRZ**) as it contains the same moiety as the building units. The synthesis of **1** in the presence of a **TRZ** guest was unsuccessful. A similar result was obtained in the presence of pyrene as a guest. Since, the π–π interactions of the transition state are pivotal for the formation of the interlocked systems, we envisioned that if the structural isomers of the building units could be used, the disruption of π–π stacking could be achieved.

We thus prepared the building units $\mathbf{L_3}$ and $\mathbf{L_4}$ (Scheme 1). Although a one-pot reaction of all four building units ($\mathbf{L_1}$–$\mathbf{L_4}$) yielded insoluble products, the reaction of $\mathbf{L_3}$ and $\mathbf{L_4}$ gave a water-soluble white precipitate (yield: 36%). The ^{1}H NMR spectrum of the product in D_2O showed broad NMR at ambient temperature (Fig. S13, ESI†). However, the ^{1}H NMR spectrum of the PF_6^- analogue in CD_3CN showed the presence of seven peaks (Fig. 3 and Fig. S14, ESI†).[25] The ^{1}H DOSY NMR spectrum showed that all peaks correspond to the same diffusion coefficient [$D = 3.98 \times 10^{-10}$ m^2 s^{-1} (log $D = -9.4$)] (Fig. S15, ESI†), which suggests the formation of a single assembly.

The NMR peaks were assigned by the ^{1}H COSY and NOESY NMR studies (Fig. S16 and S17, ESI†) which did not show any evidence of interlocked cage formation and the peaks could be readily assigned to those of a free cage. The NMR spectrum of the bromide-analogue (as formed) of the free-cage (**2**) in DMSO-d_6 was concomitant to that obtained after PF_6^- conversion (Fig. S11, ESI†). All of these observations led us to believe that in water multiple isomers of the imidazolium cage existed which leads to the broadness of NMR. Variable temperature (VT) ^{1}H NMR of the system in D_2O was then taken (Fig. S13, ESI†), which clearly showed a sharpening of the peaks as the temperature increased. It also suggested that the rate of interconversion of isomers is largely dependent on the solvent used (Fig. S13 and S19, S20, ESI†). A higher degree of the interaction of water with the imidazolium unit due to H-bonding caused broad NMR at room temperature. The interconversion is faster in DMSO and even faster in acetonitrile leading to time averaged sharp ^{1}H NMR signals in these solvents. ^{13}C NMR of the bromide analogue in DMSO-d_6 also did not show peak splitting and could be assigned to that of a free cage (Fig. S12, ESI†). To further prove the formation of an non-interlocked cage, the ESI-MS spectrum of the PF_6^- analogue was recorded in acetonitrile. The spectrum showed peaks at m/z = 299.1297 corresponding to the fragments $[M']^{3+}$ (where M′ = molar mass of $\mathbf{2}^{3+}$) with proper isotopic distribution patterns (Fig. 3 and Fig. S21, S22, ESI†). Both NMR and ESI-MS confirm the formation of the non-interlocked cage (**2**) employing the positional isomers $\mathbf{L_3}$ and $\mathbf{L_4}$ of the building blocks $\mathbf{L_1}$ and $\mathbf{L_2}$, respectively.

To examine why the meta isomers could not form an interlocked structure, a hypothetical interlocked cage and the free cage (**2**) were constructed and optimized computationally at the B3LYP/6-31G level (Fig. 3 and Fig. S26, S27, ESI†). The optimized structure of the hypothetical interlocked cage showed the rotation of the benzene rings connected to the triazine core due to steric hinderance between the benzene hydrogen and imidazolium hydrogen. This loss of planarity of the benzene rings twists the triazine core, which leads to an unfavourable π–π stacking of the triazine cores (Fig. S28, ESI†). Such an unfavourable interaction must also be present in the transition state, which leads to the selective formation of the

non-interlocked analogue. Optimizing the structure of the free cage (**2**) showed that multiple constitutional isomers were possible based on the free rotation of the benzene ring around the C–C bond connecting the triazine core to the benzene core (Fig. S26, ESI†). These constitutional isomers had similar orbital energy, which suggests the ready conversion of one to another at room temperature, which is a probable reason for the broad NMR in D_2O at room temperature.

In conclusion, the present report unlocks a new strategy of constructing a stable water-soluble imidazolium interlocked cage (**1**) without the help of dynamic covalent chemistry. The cage **1** represents a unique example of an interlocked imidazolium organic cage and it shows the phenomenon of cage swelling due to interpenetration. We also show the role of π–π stacking in interlocked cage formation and how changing the steric environment of the building blocks can lead to a non-interlocked cage (**2**). This strategy of using positional isomers of the building units to selectively synthesise the interlocked or non-interlocked form is unique in the charged cyclophane systems and brings greater understanding of the mechanism of cyclophane formation. We envision that more functionally diverse water-soluble interlocked systems can be designed by this strategy for fabricating suitable molecular hosts and smart materials.

P. S. M. thanks the CSIR-India for financial support as a research grant. The authors thank Mr Soumalya Bhattacharya for help in recording mass spectra, Mr Selva Kumar S. for help in low temperature NMR experiments and Dr Atul Kumar and Miss Prioti Choudhury Purba for fruitful discussion. All authors contributed in writing this manuscript, and they have approved the final version.

Conflicts of interest

There are no conflicts to declare.

Notes and references

1 (*a*) W.-X. Gao, H.-J. Feng, B.-B. Guo, Y. Lu and G.-X. Jin, *Chem. Rev.*, 2020, **120**, 6288; (*b*) J. F. Stoddart, *Angew. Chem., Int. Ed.*, 2017, **56**, 11094; (*c*) A. W. Heard and S. M. Goldup, *ACS Cent. Sci.*, 2020, **6**, 117.
2 B. Hudson and J. Vinograd, *Nature*, 1967, **216**, 647.
3 S. Kamitori, *J. Am. Chem. Soc.*, 1996, **118**, 8945.
4 (*a*) J. Singh, D. H. Kim, E.-H. Kim, H. Kim, R. Hadiputra, J. Jung and K.-W. Chi, *J. Am. Chem. Soc.*, 2020, **142**, 9327; (*b*) J. F. Stoddart, *Nano Lett.*, 2020, **20**, 5597.
5 (*a*) L.-L. Dang, H.-J. Feng, Y.-J. Lin and G.-X. Jin, *J. Am. Chem. Soc.*, 2020, **142**, 18946; (*b*) A. Goswami, S. Saha, P. K. Biswas and M. Schmittel, *Chem. Rev.*, 2020, **120**, 125.
6 (*a*) Y. Wang, Y. Zhang, Z. Zhou, R. T. Vanderlinden, B. Li, B. Song, X. Li, L. Cui, J. Li, X. Jia, J. Fang, C. Li and P. J. Stang, *Nat. Commun.*, 2020, **11**, 2727; (*b*) Y. Sun, C. Chen and P. J. Stang, *Acc. Chem. Res.*, 2019, **52**, 802; (*c*) H. Sepehrpour, W. Fu, Y. Sun and P. J. Stang, *J. Am. Chem. Soc.*, 2019, **141**, 14005.
7 (*a*) Y. Sun, C. Chen, J. Liu and P. J. Stang, *Chem. Soc. Rev.*, 2020, **49**, 3889; (*b*) Y. Qin, X. Liu, P.-P. Jia, L. Xu and H.-B. Yang, *Chem. Soc. Rev.*, 2020, **49**, 5678; (*c*) W.-J. Li, Z. Hu, L. Xu, X.-Q. Wang, W. Wang, G.-Q. Yin, D.-Y. Zhang, Z. Sun, X. Li, H. Sun and H.-B. Yang, *J. Am. Chem. Soc.*, 2020, **142**, 16748.
8 (*a*) Y. Li, G.-F. Huo, B. Liu, B. Song, Y. Zhang, X. Qian, H. Wang, G.-Q. Yin, A. Filosa, W. Sun, S. W. Hla, H.-B. Yang and X. Li, *J. Am. Chem. Soc.*, 2020, **142**, 14638; (*b*) M. Yoshizawa and L. Catti, *Acc. Chem. Res.*, 2019, **52**, 2392; (*c*) N. Noto, Y. Hyodo, M. Yoshizawa, T. Koike and M. Akita, *ACS Catal.*, 2020, **10**, 14283; (*d*) H. Zhu, Q. Li, B. Shi, H. Xing, Y. Sun, S. Lu, L. Shangguan, X. Li, F. Huang and P. J. Stang, *J. Am. Chem. Soc.*, 2020, **142**, 17340.
9 (*a*) A. D. Gill, B. L. Hickey, W. Zhong and R. J. Hooley, *Chem. Commun.*, 2020, **56**, 4352; (*b*) J. Zhou, Y. Zhang, G. Yu, M. R. Crawley, C. R. P. Fulong, A. E. Friedman, S. Sengupta, J. Sun, Q. Li, F. Huang and T. R. Cook, *J. Am. Chem. Soc.*, 2018, **140**, 7730; (*c*) T. R. Cook and P. J. Stang, *Chem. Rev.*, 2015, **115**, 7001.
10 G. Zhang, O. Presly, F. White, I. M. Oppel and M. Mastalerz, *Angew. Chem., Int. Ed.*, 2014, **53**, 5126.
11 (*a*) T. Hasell, X. Wu, J. T. A. Jones, J. Bacsa, A. Steiner, T. Mitra, A. Trewin, D. J. Adams and A. I. Cooper, *Nat. Chem.*, 2010, **2**, 750; (*b*) K. Acharyya and P. S. Mukherjee, *Angew. Chem., Int. Ed.*, 2019, **58**, 8640; (*c*) R. McCaffrey, H. Long, Y. Jin, A. Sanders, W. Park and W. Zhang, *J. Am. Chem. Soc.*, 2014, **136**, 1782.
12 A. Dey, S. Chand, L. O. Alimi, M. Ghosh, L. Cavallo and N. M. Khashab, *J. Am. Chem. Soc.*, 2020, **142**, 15823.
13 K. S. Chichak, S. J. Cantrill, A. R. Pease, S.-H. Chiu, G. W. V. Cave, J. L. Atwood and J. F. Stoddart, *Science*, 2004, **304**, 1308.
14 Z. Cui, Y. Lu, X. Gao, H.-J. Feng and G.-X. Jin, *J. Am. Chem. Soc.*, 2020, **142**, 13667.
15 S. Xu, P. Li, Z.-Y. Li, C. Yu, X. Liu, Z. Liu and S. Zhang, *CCS Chem.*, 2020, 1838.
16 (*a*) A. Kumar and P. S. Mukherjee, *Chem. – Eur. J.*, 2020, **26**, 4842; (*b*) M. Fujita, D. Oguro, M. Miyazawa, H. Oka, K. Yamaguchi and K. Ogura, *Nature*, 1995, **378**, 469.
17 H. Gan, N. Xu, C. Qin, C. Sun, X. Wang and Z. Su, *Nat. Commun.*, 2020, **11**, 4103.
18 T. K. Ronson, Y. Wang, K. Baldridge, J. S. Siegel and J. R. Nitschke, *J. Am. Chem. Soc.*, 2020, **142**, 10267.
19 E. J. Dale, N. A. Vermeulen, M. Juríček, J. C. Barnes, R. M. Young, M. R. Wasielewski and J. F. Stoddart, *Acc. Chem. Res.*, 2016, **49**, 262.
20 (*a*) D. Xia, P. Wang, X. Ji, N. M. Khashab, J. L. Sessler and F. Huang, *Chem. Rev.*, 2020, **120**, 6070; (*b*) X.-L. Chen, Y.-J. Shen, C. Gao, J. Yang, X. Sun, X. Zhang, Y.-D. Yang, G.-P. Wei, J.-F. Xiang, J. L. Sessler and H.-Y. Gong, *J. Am. Chem. Soc.*, 2020, **142**, 7443; (*c*) Y. Li, K. M. Mullen, T. D. W. Claridge, P. J. Costa, V. Felix and P. D. Beer, *Chem. Commun.*, 2009, 7134.
21 A. B. Aletti, A. Miljkovic, L. Toma, R. Bruno, D. Armentano, T. Gunnlaugsson, G. Bergamaschi and V. Amendola, *J. Org. Chem.*, 2019, **84**, 4221.
22 C. Zhang, T. Jiao, L. Tong, H. Wang, Y. Pan and H. Li, *Chem. Commun.*, 2020, **56**, 3903.
23 Y.-W. Zhang, S. Bai, Y.-Y. Wang and Y.-F. Han, *J. Am. Chem. Soc.*, 2020, **142**, 13614.
24 P. Li, S. Xu, C. Yu, Z.-Y. Li, J. Xu, Z.-M. Li, L. Zou, X. Leng, S. Gao, Z. Liu, X. Liu and S. Zhang, *Angew. Chem., Int. Ed.*, 2020, **59**, 7113.
25 In ^{1}H NMR of 2(PF_6), the imidazolium proton (Hg) (Fig. S14, ESI†) has less integration value than expected; this can be attributed to the acidic nature of the proton which leads to H/D exchange, and this can be proved by its mass spectrum in CD_3CN where the most intense peak is shifted by a value of 2/*z* (*z* being the charge of the fragment) (Fig. S23, ESI†), indicating the presence of 2 deuterium atoms in the backbone of the cage. The same argument should also hold true for the imidazolium proton of 1(Br) in D_2O and 2(Br) in DMSO-d_6 and D_2O, which also show lower integration values (Fig. S1 and S11, ESI†).

